

Three Gauge-Boson Production in  $e^-e^-$  Collisions in the  
Left-Right Model

LR-Report 4

Aarre Pietilä

Department of Applied Physics, University of Turku

Jukka Maalampi

Department of Theoretical Physics, University of Helsinki

December 1993

### Abstract

The new linear colliders (CLIC, NLC, JLC, TESLA) can be constructed to produce  $e^- e^-$  collisions in the c.m. energy range of 1 – 2 TeV. In the present work, the production of a same-signed W-boson pair along with a neutral Z-boson in electron-electron collisions has been investigated in the framework of the classic left-right symmetric electroweak model in this energy region. These production channels arise on one hand due to the Majorana neutrinos and the doubly charged Higgs boson of the model and on the other hand due to the mixing of the gauge bosons  $W_L$  and  $W_R$ .

The cross sections are proportional to  $(mK)^2$ , where  $m$  refers to the mass of the heavy neutrino, and the parameter  $K$  is given by  $K = \cos^2 \zeta$  for the heavy W-pair,  $K = \sin \zeta \cos \zeta$  for the light and heavy pair,  $K = \sin^2 \zeta$  for the light pair, and  $\zeta$  is the W mixing angle. If  $\zeta$  obeys its upper limit estimate (around 0.001) found in the literature and the particles have their masses in the region considered by us, only the production of a heavy W pair with a Z-boson may play some role in experiments.

According to our numerical calculations the total cross section in the case of a light Z is of the order of 2 fbarn at 2 TeV and about nine times greater at 4 TeV, when the W mass is 0.5 TeV and the heavy neutrino mass 1 TeV. The cross sections can be greatly enhanced if the doubly charged Higgs lies at the neighbourhood of these energies. On the other hand we expect the increase of the W mass would decrease the cross section in the ratio  $(0.5TeV/M_W)^4$ .

# Contents

<b>1</b>	<b>Introduction</b>	<b>2</b>
<b>2</b>	<b>Formulas</b>	<b>4</b>
2.1	Calculation of vertices . . . . .	4
2.2	Amplitudes . . . . .	7
<b>3</b>	<b>Cross sections</b>	<b>16</b>
<b>4</b>	<b>Numerical results and discussion</b>	<b>21</b>
<b>A</b>	<b>Figures of Chapter 4</b>	<b>25</b>

# Chapter 1

## Introduction

Many attempts have been made to extend the standard electroweak model to a theory possessing a left-right symmetry. Among the schemes considered most attractive is perhaps the classic model of Pati, Salam and Mohapatra [13], which is based on the gauge group  $SU(2)_L \times SU(2)_R \times U(1)_{B-L}$ . In this model left- and right-handed fermion fields accommodate doublets of  $SU(2)_L$  and  $SU(2)_R$  symmetry, respectively. The breaking of the gauge symmetry, following the chain  $SU(2)_L \times SU(2)_R \times U(1)_{B-L} \rightarrow SU(2)_L \times U(1)_Y \rightarrow U(1)_{em}$ , can be arranged by introducing to the theory a bidoublet Higgs field  $\Phi$  transforming as  $\Phi = (\mathbf{2}, \mathbf{2}, 0)$  and a "right-handed" triplet field  $\Delta_R$  transforming as  $\Delta_R = (\mathbf{1}, \mathbf{3}, 2)$ . The triplet Higgs having both  $SU(2)_R$  and  $U(1)_{B-L}$  charge takes care of the first step of the symmetry breaking. Its vacuum expectation value sets the mass scale of the "right-handed" gauge bosons, which is according to experiments most probably above 0.5 TeV. One could in the left-right symmetric model (LRM) use instead of the triplet also a field transforming as a doublet under  $SU(2)_R$  and having a non-vanishing  $B-L$ . The triplet field has, however, an extra benefit which makes it a more natural choice. It couples to  $|\Delta L| = 2$  lepton currents through the Yukawa coupling  $ih_R \Psi_R^T C \tau_2 \Delta_R \Psi_R$  giving rise to Majorana mass terms for right-handed neutrinos. This leads to the see-saw mechanism of neutrino masses according to which there are in each fermion family two Majorana neutrinos, one very light and another very heavy. Apart of the lepton number violation, a central prediction of the left-right symmetric model is the existence of a extra heavy Majorana neutrino, which is a superposition of the ordinary isodoublet left-handed neutrino and a isosinglet right-handed neutrino.

So far there are no direct experimental evidences of the left-right symmetric model; no right-handed interactions have been discovered and experimental data does not make difference between Dirac and Majorana neutrinos. It will be one of the challenges of the next generation accelerators to look for evidences of the left-right symmetry in various high-energy processes. Especially the new linear colliders, such as CLIC, JLC, NLC and TESLA, which are planned to start operating in the beginning of the 21th century at 0.5-2 TeV energy, can be made, besides the  $e^+e^-$  mode, capable to produce high-energy  $e^-e^-$  collisions. These high-energy electron-electron collisions would provide a new and an important method to investigate various extensions of the Standard Model of the electroweak interactions. The phenomenological implications of the  $\Delta L = 2$  interactions and the see-saw mechanism in  $e^-e^-$  collisions have been recently investigated [16],[14], [8],[9],[6],[3].

In our previous papers [12],[14],[15] we considered the pair production of the charged gauge bosons from  $e^+e^-$  and  $e^-e^-$  collisions in the framework of the classic left-right symmetric model (LRM). Our main motivation was to find out if the measurement of the W-production cross sections could allow for estimating the order of the magnitude of the mass of the heavy neutrino. This would cast light on the fundamental question of whether neutrinos are Dirac or Majorana particles.

Our conclusions, however, were in this respect not very encouraging, because the heavy neutrino turned out to have a negligible effect on production of the light W pair in the  $e^+e^-$  annihilation and even the production rate of the light-heavy pair was negligible both in the annihilation channel and in the  $e^-e^-$  collisions due to their dependence on the small mixing of  $W_L$  and  $W_R$ . In addition, the

# Chapter 2

## Formulas

### 2.1 Calculation of vertices

The matter of the LRM contains one left-handed and one right-handed doublet of the gauge group  $SU(2)_L \times SU(2)_R \times U(1)_{B-L}$  for the electron family,

$$\Psi_L = \begin{pmatrix} \nu_e \\ e^- \end{pmatrix}_L = (\mathbf{2}, \mathbf{0}, -1), \quad \Psi_R = \begin{pmatrix} \nu_e \\ e^- \end{pmatrix}_R = (\mathbf{0}, \mathbf{2}, -1), \quad (2.1)$$

and similarly for other families. In order to generate masses for fermions one needs at least one Higgs bidoublet

$$\Phi = \begin{pmatrix} \phi_1^0 & \phi_1^+ \\ \phi_2^- & \phi_2^0 \end{pmatrix} = (\mathbf{2}, \mathbf{2}, 0), \quad (2.2)$$

whose vacuum expectation value (VEV) is given by

$$\langle \Phi \rangle = \frac{1}{\sqrt{2}} \begin{pmatrix} K_1 & 0 \\ 0 & K_2 \end{pmatrix}. \quad (2.3)$$

Here  $K_1$  and  $K_2$  are in general complex, but if we assume that the explicit CP violation is small we can take them real [2]. In order to break the symmetry to the electromagnetic group additional Higgs multiplets with  $B-L \neq 0$  are needed. To introduce at the same time Majorana mass terms for the neutrinos we add to the theory the triplets

$$\begin{aligned} \Delta_L &= \vec{\delta}_L \cdot \vec{\tau} = \begin{pmatrix} \delta_L^+ & \sqrt{2}\delta_L^{++} \\ \sqrt{2}\delta_L^0 & -\delta_L^+ \end{pmatrix} = (\mathbf{3}, \mathbf{1}, 2), \\ \Delta_R &= \vec{\delta}_R \cdot \vec{\tau} = \begin{pmatrix} \delta_R^+ & \sqrt{2}\delta_R^{++} \\ \sqrt{2}\delta_R^0 & -\delta_R^+ \end{pmatrix} = (\mathbf{1}, \mathbf{3}, 2) \end{aligned} \quad (2.4)$$

with the VEV's given by

$$\langle \Delta_{L,R} \rangle = \frac{1}{\sqrt{2}} \begin{pmatrix} 0 & 0 \\ v_{L,R} & 0 \end{pmatrix}. \quad (2.5)$$

There are all together seven vector bosons:  $W_{L,R}^\pm = \frac{1}{\sqrt{2}}(V_{L,R}^1 \pm iV_{L,R}^2)$ ,  $V_{L,R}^3$ , and  $B$ . We define the physical states of the bosons by the equations

$$\begin{pmatrix} W_L^\pm \\ W_R^\pm \end{pmatrix} = \begin{pmatrix} \cos \zeta & -\sin \zeta \\ \sin \zeta & \cos \zeta \end{pmatrix} \begin{pmatrix} W_1^\pm \\ W_2^\pm \end{pmatrix}, \quad (2.6)$$

$$\begin{pmatrix} V_L^3 \\ V_R^3 \\ B \end{pmatrix} = (R_{ij}) \begin{pmatrix} Z_1 \\ Z_2 \\ Z_3 = \gamma \end{pmatrix} \quad (i = L, R, B). \quad (2.7)$$

the kinetic energy of the Higgs doublet

$$\mathcal{L}_{kin}^\phi = \text{Tr}\{(D_\mu \Phi)^\dagger (D^\mu \Phi)\} \quad (2.16)$$

where

$$D_\mu \Phi = \partial_\mu \Phi - \frac{i}{2}(g_L \vec{\tau} \cdot \vec{V}_{L\mu} \Phi - g_R \Phi \vec{\tau} \cdot \vec{V}_{R\mu}) \quad (2.17)$$

giving as its relevant part

$$- \frac{g_L g_R}{2} \cos \zeta \{R_{Ll} W_2^- [K_1 (\Phi_1^+)^\dagger - K_2 \Phi_2^-] + R_{Rl} W_1^- [K_1 \Phi_2^- - K_2 (\Phi_1^+)^\dagger]\} Z_l + \dots \quad (2.18)$$

In these equations we have used the Cartesian components of the vector bosons and of the triplet Higgses. For the various coupling constants appearing in the formulas we have the following expressions

$$\Gamma_{lj}^\mu = G_{lj}^L \gamma^\mu \frac{1 - \gamma_5}{2} + G_{lj}^R \gamma^\mu \frac{1 + \gamma_5}{2}, \quad (2.19)$$

$$G_{lj}^L = \frac{g_L}{\sqrt{2}} \begin{pmatrix} \cos \eta \cos \zeta & \sin \eta \cos \zeta \\ -\cos \eta \sin \zeta & -\sin \eta \sin \zeta \end{pmatrix}, \quad (2.20)$$

$$G_{lj}^R = \frac{g_R}{\sqrt{2}} \begin{pmatrix} -\sin \eta \sin \zeta & \cos \eta \sin \zeta \\ -\sin \eta \cos \zeta & \cos \eta \cos \zeta \end{pmatrix},$$

$$-e_{ll'l''} = \begin{cases} (\cos \zeta)^2 g_L R_{Ll'l''} + (\sin \zeta)^2 g_R R_{Rl'l''}, & l = l' = 1 \\ (\sin \zeta)^2 g_L R_{Ll'l''} + (\cos \zeta)^2 g_R R_{Rl'l''}, & l = l' = 2 \\ \sin \zeta \cos \zeta (g_R R_{Rl'l''} - g_L R_{Ll'l''}), & l \neq l', \end{cases} \quad (2.21)$$

$$G^A(\nu_j \nu_{j'} Z_l) = \begin{cases} \frac{1}{4} [g_L \cos^2 \eta R_{Ll} - g_R \sin^2 \eta R_{Rl} - g' (\cos^2 \eta - \sin^2 \eta) R_{Al}], & j = j' = 1 \\ \frac{1}{4} [g_L R_{Ll} + g_R R_{Rl} - g' R_{Al}] \cos \eta \cdot \sin \eta, & j \neq j' \\ \frac{1}{4} [g_L \sin^2 \eta R_{Ll} - g_R \cos^2 \eta R_{Rl} + g' (\cos^2 \eta - \sin^2 \eta) R_{Al}], & j = j' = 2, \end{cases} \quad (2.22)$$

and

$$\begin{cases} G^V(eeZ_l) = (-\frac{1}{4} g_L R_{Ll} - \frac{1}{4} g_R R_{Rl} - \frac{1}{2} g' R_{Al}) \\ G^A(eeZ_l) = (-\frac{1}{4} g_L R_{Ll} + \frac{1}{4} g_R R_{Rl}) \end{cases} \quad (2.23)$$

We will also need the right-handed coupling constant

$$G^R(eeZ) = G^V(eeZ_l) - G^A(eeZ_l) = -\frac{1}{2}(g_R R_{Rl} + g' R_{Al}). \quad (2.24)$$

The above equations are given for a general case. Neglecting the  $W_L - W_R$  mixing and the  $\nu_L - \nu_R$  mixing and setting  $\eta = 0 = \zeta$ , and using for the coupling constants the approximation  $g_L \approx g_R \approx g$  we obtain in the most important case ( $\nu_j = \nu_2$ ,  $W_l = W_{l'} = W_2$ ) the following more simple expressions:

$$\begin{cases} \Gamma_{22}^\mu = \frac{g}{2\sqrt{2}} \gamma^\mu (1 + \gamma_5) = G_{enW} \gamma^\mu (1 + \gamma_5) \\ 2 \Gamma_{22l}^\mu = -\frac{1}{2} (g R_{Rl} - g' R_{Al}) \gamma^\nu \gamma^5 = G_{nnZ} \gamma^\nu \gamma^5 \\ e_{22l} = -g_R R_{Rl} = -G_{WWZ} \\ G_{22}^R = \frac{g_R}{\sqrt{2}} = 2 G_{enW}. \end{cases} \quad (2.25)$$

$i$	1	2	3	4	5	6
$\lambda_1 \lambda_2 \lambda_3$	$\mu_1 \mu_2 \mu_3$	$\mu_2 \mu_3 \mu_1$	$\mu_3 \mu_1 \mu_2$	$\mu_2 \mu_1 \mu_3$	$\mu_1 \mu_3 \mu_2$	$\mu_3 \mu_2 \mu_1$
$\Gamma_1$	$\Gamma^C(e\nu W_1)$	$\Gamma^C(e\nu_2 W_2)$	$\Gamma^C(eeZ)$	$\Gamma^C(e\nu W_2)$	$\Gamma^C(e\nu_2 W_1)$	$\Gamma^C(eeZ)$
$S_1$	$S_\nu(k_1 - p_2)$	$S_{\nu_2}(k_2 - p_2)$	$S_e^C(p_2 - k_3)$	$S_\nu(k_2 - p_2)$	$S_{\nu_2}(k_1 - p_2)$	$S_e^C(p_2 - k_3)$
$\Gamma_2$	$\Gamma(e\nu W_2)$	$\Gamma(\nu_1 \nu_2 Z) + \Gamma^C$	$\Gamma^C(e\nu W_1)$	$\Gamma(e\nu W_1)$	$\Gamma(\nu_1 \nu_2 Z) + \Gamma^C$	$\Gamma^C(e\nu W_2)$
$S_2$	$S_e(p_1 - k_3)$	$S_{\nu_1}(p_1 - k_1)$	$S_\nu^C(k_2 - p_1)$	$S_e(p_1 - k_3)$	$S_{\nu_1}(p_1 - k_2)$	$S_\nu^C(k_1 - p_1)$
$\Gamma_3$	$\Gamma(eeZ)$	$\Gamma(e\nu_1 W_1)$	$\Gamma(e\nu W_2)$	$\Gamma(eeZ)$	$\Gamma(e\nu_1 W_2)$	$\Gamma(e\nu W_1)$
$q_1$	$k_1 - p_2$	$k_2 - p_2$	$k_3 - p_2$	$k_2 - p_2$	$k_1 - p_2$	$k_3 - p_2$
$q_2$	$p_1 - k_3$	$p_1 - k_1$	$p_1 - k_2$	$p_1 - k_3$	$p_1 - k_2$	$p_1 - k_1$
$m_1$	$m_\nu$	$m_{\nu_2}$	$m_e$	$m_\nu$	$m_{\nu_2}$	$m_e$
$m_2$	$m_e$	$m_{\nu_1}$	$m_\nu$	$m_e$	$m_{\nu_1}$	$m_\nu$

Table 2.1: The expressions for the various quantities appearing in the amplitudes corresponding to the diagrams a)-b) of Fig 2.1.

In table 2.1 we summarize the expressions for the quantities  $\Gamma$  and  $S$  for the six amplitudes corresponding to the diagrams of Fig 2.2 and their variations.

The numerator of the every term  $T^{\lambda_1 \lambda_2 \lambda_3}$  has the decomposition

$$\begin{aligned}
& (G_1^V + G_1^A \gamma_5) \gamma^{\lambda_1} (\not{h}_1 + m_1) (G_2^V + G_2^A \gamma_5) \gamma^{\lambda_2} (\not{h}_2 + m_2) (G_3^V + G_3^A \gamma_5) \gamma^{\lambda_3} \\
= & (V_5 + A_5 \gamma_5) \tau_5^{\lambda_1 \lambda_2 \lambda_3} (q_1, q_2) + m_1 m_2 (V_3 + A_3 \gamma_5) \tau_3^{\lambda_1 \lambda_2 \lambda_3} \\
& + m_2 (V_{4,1} + A_{4,1} \gamma_5) \tau_{4,1}^{\lambda_1 \lambda_2 \lambda_3} (q_1) + m_1 (V_{4,2} + A_{4,2} \gamma_5) \tau_{4,2}^{\lambda_1 \lambda_2 \lambda_3} (q_2)
\end{aligned} \tag{2.33}$$

where we have used the notations

$$\left\{ \begin{array}{l}
V_5 = G_1^V G_2^V G_3^V + G_1^V G_2^A G_3^A + G_2^V G_1^A G_3^A + G_3^V G_1^A G_2^A = V(+, +, +) \\
A_5 = G_1^A G_2^A G_3^A + G_1^A G_2^V G_3^V + G_2^A G_1^V G_3^V + G_3^A G_1^V G_2^V = V(-, -, -) \\
\tau_5 = \gamma^{\lambda_1} \not{h}_1 \gamma^{\lambda_2} \not{h}_2 \gamma^{\lambda_3} \\
\tau_3 = m_1 m_2 [V(+, -, -) + A(+, -, -) \gamma_5] \gamma^{\lambda_1} \gamma^{\lambda_2} \gamma^{\lambda_3} \\
\tau_{4,2}(q_2) = m_1 [V(+, -, +) + A(+, -, +) \gamma_5] \gamma^{\lambda_1} \gamma^{\lambda_2} \not{h}_2 \gamma^{\lambda_3} \\
\tau_{4,1}(q_1) = m_2 [V(+, +, -) + A(+, +, -) \gamma_5] \gamma^{\lambda_1} \not{h}_1 \gamma^{\lambda_2} \gamma^{\lambda_3}
\end{array} \right. \tag{2.34}$$

From the graphs c), d), e) and f) of Fig 2.2 we obtain the amplitude

which is equal to

$$i^5 \bar{\nu}(2) \Gamma_{j1C}^\mu S_j(p_1 - k_2) \Gamma_{jl_2}^{\mu_2} u(1). \quad (2.40)$$

The other terms of (2.35) have been obtained in the similar way. We note that the s-channel graphs e) and f) balance the t-channel graphs c) and d), respectively. If we take off in the graphs c) and e) the part where the  $W$  decays into the  $Z$  and  $W$  bosons the remains give the amplitude for the process  $e^- e^- \rightarrow W^- W^-$ . In the graphs d) and f) we see at the lower level the process  $e^- e^- \rightarrow \Delta^{--} Z$ .

The graph g) with its alternatives produce our last amplitude

$$\begin{aligned} T^{\mu_1 \mu_2 \mu_3} &= [\Gamma_{jl_2 C}^{\mu_2} S_j(k_2 - p_2) \Gamma_{jk}^- + \Gamma_{jk C}^- S_{jC}(k_2 - p_1) \Gamma_{jl_2}^{\mu_2}] \cdot D^{\Phi_k^-}(k_1 + k_3) F_{l_1 l_3 \Phi_k^-}^{\mu_1 \mu_3} \\ &+ [\Gamma_{jl_1 C}^{\mu_1} S_j(k_1 - p_2) \Gamma_{jk}^- + \Gamma_{jk C}^- S_{jC}(k_1 - p_1) \Gamma_{jl_1}^{\mu_1}] \cdot D^{\Phi_k^-}(k_2 + k_3) F_{l_2 l_3 \Phi_k^-}^{\mu_2 \mu_3} \end{aligned} \quad (2.41)$$

This amplitude is, however, negligible compared with the other amplitudes.

Deshpande et al [2] have recently pointed out that the phenomenology of the Higgs sector depends crucially on the order of the three coupling constants  $\beta_i$  in the general Higgs potential. If we want to have neutrinos as Majorana particles and preserve the see-saw mechanism and at the same time keep the extra Higgs particles and gauge bosons light enough to be accesible for the near future accelerators, this will demand in the case of the non-vanishing couplings  $\beta_i$  a fine-tuning of these parameters at least to the order of  $10^{-7}$ . But if we constrain  $\beta$ 's to vanish by some symmetry beyond the classic LRM, the mass scales  $v_L$  and  $v_R$  are disconnected and there remains a remnant see-saw relation, which is most naturally satisfied by the condition  $v_L = 0$ .

Deshpande et al [2] have given the mass matrices of the Higgses in the case  $\beta_i = v_L = 0$ . In these scenarios the linear combination  $K_1 \phi_2^- - K_2 (\phi_1^+)^\dagger$  and another combination, which predominatly is  $\delta_R^-$ , are Goldstone fields and they will be eaten by the negatively charged  $W$  bosons. So, only the combination  $K_2 \phi_2^- - K_1 (\phi_1^+)^\dagger$  of the bidoublet Higgses will mediate in our process. Gunion et al [5] have presented a simple model, which can be retrieved from the models treated by Deshpande et al by constraining further the potential couplings and putting  $K_2 = 0$ . Such a model is still phenomenologically acceptable. The conditon  $K_2 = 0$ , however, would mean that the right-handed and the left-handed vector bosons do not mix. If we neglect the left-handed triplet, too, we are left with only one positively charged Higgs  $h^+$ , which is mainly  $\phi_1^+$ , and is now a mass eigen state. We have given the couplings of  $\phi_1^+$ , which can be read in the formulas (2.14) and (2.18), in the Fig. 2. According to these rules the amplitude of the graph g) is proportional to the masses  $m_e$  and  $m_D$ , and thus negligibel. Here we have utilized the fact that in the LRM the electron mass has been given by

$$m_e = \frac{fK_2 + gK_1}{\sqrt{2}} \quad (2.42)$$

and that the neutrino has the Dirac mass given by

$$m_D = \frac{fK_1 + gK_2}{\sqrt{2}}. \quad (2.43)$$

The smallnes of the  $m_D$  mass can be seen by expressing it in terms of the mass eigenvalues  $m_i$  and of the mixing angle  $\eta$  of the neutrinos:

$$m_D = \frac{1}{2}(m_1 + m_2) \sin 2\eta. \quad (2.44)$$

We note that here and anywhere in this paper the masses  $m_i$  refer to the eigenvalues of the neutrinos' mass matrix and the real mass of the  $\nu_1$ -neutrino is  $m_{\nu_1} = -m_1$  in this model. We also note that, because the  $\delta_R^-$  has not totally been eaten by a  $W$ -boson we would actually have instead of the graph g) two new graphs: one with  $h^-$  in the place of the  $\phi^-$  in the graph g) and another in the s-channel with  $h^-$  in one of the virtual  $\Delta^{--}$  in the graph f) and  $Z$  interchanged with one

where

$$c = -2m_2 G_{enW}^2 = -\frac{m_2 g_R^2}{4} \quad (2.46)$$

Similarly in the formula (2.35), the only important terms are those proportional to the heavy neutrino mass. For example, from the first and second term (arising from the graph c)) we get

$$e_{l_1, l_2, l_3} \cdot m_j \left[ \frac{\Gamma_{jl_2}^{\mu_2} \Gamma_{jl}^{\mu_1}}{(k_2 - p_2)^2 - m_j^2} + \frac{\Gamma_{jl}^{\mu_1} \Gamma_{jl_2}^{\mu_2}}{(k_2 - p_1)^2 - m_j^2} \right] \cdot D_{\mu\nu}^{Wl}(k_1 + k_3) F^{\mu_1 \nu \mu_3}(k_1, k_1 - k_3, k_3), \quad (2.47)$$

where  $j = 2$ . By using here the identity  $\gamma^\mu \gamma^{\mu_2} = 2 g^{\mu \mu_2} - \gamma^{\mu_2} \gamma^\mu$  we obtain from a  $g^{\mu \mu_2}$ -part a term which can be related to the similar expression of the diagram e). Further, we give the terms corresponding the exchange of the W-bosons as separate amplitudes. The diagram d) also gives a rise to two amplitudes corresponding to the different substitutions of the delta Higgs into the vertices. This arrangement gives the following amplitudes

$$T_7 = -c \cdot G_{WWZ} \left[ \frac{1}{t_2 - m_2^2} - \frac{1}{u_1 - m_2^2} \right] \cdot D_{\mu\nu}^{W_2}(k_1 + k_3) F^{\mu_1 \nu \mu_3}(k_1, k_1 - k_3, k_3) (1 + \gamma_5) \gamma^{\mu_2} \gamma^\mu, \quad (2.48)$$

$$T_8 = -c \cdot G_{WWZ} \left[ \frac{1}{u_2 - m_2^2} - \frac{1}{t_1 - m_2^2} \right] \cdot D_{\mu\nu}^{W_2}(k_2 + k_3) F^{\mu_2 \nu \mu_3}(k_2, k_2 - k_3, k_3) (1 + \gamma_5) \gamma^{\mu_1} \gamma^\mu, \quad (2.49)$$

$$T_9 = -2c \cdot G_{WWZ} \left[ \frac{1}{u_1 - m_2^2} + \frac{2}{s - M_\Delta^2} \right] \cdot D_{\mu\nu}^{W_2}(k_1 + k_3) F^{\mu_1 \nu \mu_3}(k_1, k_1 - k_3, k_3) (1 + \gamma_5) g^{\mu \mu_2}, \quad (2.50)$$

$$T_{10} = -2c \cdot G_{WWZ} \left[ \frac{1}{t_1 - m_2^2} + \frac{2}{s - M_\Delta^2} \right] \cdot D_{\mu\nu}^{W_2}(k_2 + k_3) F^{\mu_2 \nu \mu_3}(k_2, k_2 - k_3, k_3) (1 + \gamma_5) g^{\mu \mu_1}, \quad (2.51)$$

$$T_{11} = 4c G_{eeZ}^R \frac{g^{\mu_1 \mu_2}}{s_3 - M_\Delta^2} \frac{\gamma^{\mu_3} (\not{p}_2 - \not{k}_3)}{t_{b3}} (1 + \gamma_5), \quad (2.52)$$

$$T_{12} = 4c G_{eeZ}^R \frac{g^{\mu_1 \mu_2}}{s_3 - M_\Delta^2} \frac{(\not{p}_1 - \not{k}_3) \gamma^{\mu_3}}{t_{a3}} (1 + \gamma_5), \quad (2.53)$$

$$T_{13} = 16c G_{eeZ}^R \frac{g^{\mu_1 \mu_2}}{s_3 - M_\Delta^2} \frac{(p_1 + p_2)^{\mu_3}}{s - M_\Delta^2} (1 + \gamma_5). \quad (2.54)$$

The symbols  $s_1, s_2, t_1, t_2$  are identical to the ones defined by E. Byckling and K. Kajantie [1], if we replace their momenta  $p_a, p_b, p_1, p_2, p_3$  with our momenta  $p_1, p_2, k_1, k_3, k_2$ , respectively. They

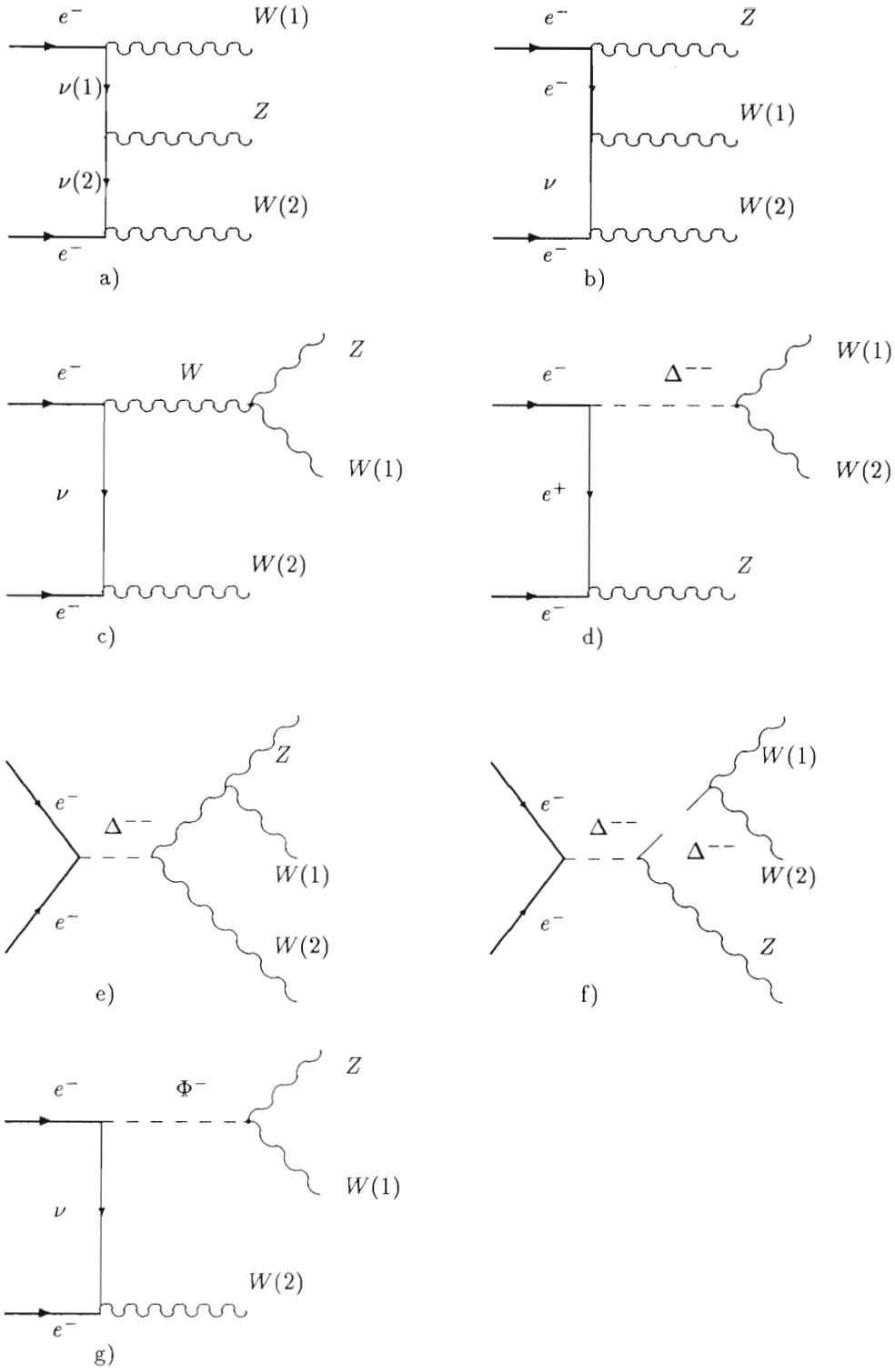


Figure 2.1: The lowest-order Feynman graphs for the process  $ee \rightarrow WWZ$

## Chapter 3

# Cross sections

The squared spin summed amplitude is of the form

$$\sum_{spins} |M|^2 = -\left(g^{\mu_1\nu_1} - \frac{k_1^{\mu_1} k_1^{\nu_1}}{M_1^2}\right) \left(g^{\mu_2\nu_2} - \frac{k_2^{\mu_2} k_2^{\nu_2}}{M_2^2}\right) \left(g^{\mu_3\nu_3} - \frac{k_3^{\mu_3} k_3^{\nu_3}}{M_3^2}\right) \cdot \text{Tr} \{T_{\mu_1\mu_2\mu_3} \not{p}_1 \gamma^0 (T_{\nu_1\nu_2\nu_3})^\dagger \gamma^0 \not{p}_2\}. \quad (3.1)$$

The total cross section of the production of the unpolarized final state  $WWZ$  in a collision of unpolarized electrons and positrons is then given by the formula

$$\sigma_3 = \frac{1}{(2\pi)^5} \frac{\int \prod_{i=1}^3 \frac{d^3 k_i}{2E_i} \delta^4(p_1 + p_2 - \sum k_i) \langle \Sigma |M|^2 \rangle}{2s} \quad (3.2)$$

with

$$\langle \Sigma |M|^2 \rangle = \frac{1}{4} \sum_{spins} |M|^2. \quad (3.3)$$

We notice that the expression (3.2) must be divided by two, if there are two identical bosons in the final state.

The total amplitude  $T$  is a sum of the partial amplitudes  $T_{ij}$ , where  $i$  refers to a diagram with the final particles in the fixed positions and  $j$  stands for the other indices related to the virtual particles in the diagram. Our computation is based on the following expansion

$$\begin{aligned} & \int \text{Tr} \{T_{\mu_1\mu_2\mu_3} \not{p}_1 \gamma^0 (T_{\nu_1\nu_2\nu_3})^\dagger \gamma^0 \not{p}_2\} \left(g^{\mu_1\nu_1} - \frac{k_1^{\mu_1} k_1^{\nu_1}}{M_1^2}\right) \dots \left(g^{\mu_3\nu_3} - \frac{k_3^{\mu_3} k_3^{\nu_3}}{M_3^2}\right) \\ &= \sum_{i_1, i_2} \sum_{j_1, j_2} \sum_n C_n(i_1 j_1, i_2 j_2) \int_{phase\ space} f(i_1 j_1) \cdot f(i_2 j_2) \text{ctr}(n, i_1 i_2) \end{aligned} \quad (3.4)$$

Here  $n$  separates, when necessary, the different parts of a given trace  $tr(i_1 j_1, i_2 j_2)$ . The symbol  $ctr$  in (3.4) is the trace contracted by the polarization factors. The coefficients  $f(ij)$  contain the denominators coming from the propagators. They are, of course, functions of the integration variables. For example, in a good approximation we can take the two neutrinos in the graph a) identical ( $j_1 = j_2$ ) and then use in the both graphs a) and b) our amplitude index  $j$  to refer to the virtual neutrino. These then yield 12 partial amplitudes  $T_{ij}$ , where  $i$  runs as the permutations of the  $\mu_1\mu_2\mu_3$  and  $j$  takes the values 1 and 2. Every partial amplitude is of the form  $G_1 S_1 \Gamma_2 S_2 \Gamma_3$  and has the expansion (2.33). We now use the relation

$$16 \cdot \Delta_4 = \begin{vmatrix} 0 & s & M_1^2 - t_1 & t_2 + s - s_1 \\ s & 0 & t_1 + s - s_2 & M_2^2 - t_2 \\ M_1^2 - t_1 & t_1 + s - s_2 & 2M_1^2 & s - s_1 - s_2 + M_3^2 \\ t_2 + s - s_1 & M_2^2 - t_2 & s - s_1 - s_2 + M_3^2 & 2M_2^2 \end{vmatrix} \quad (3.9)$$

$$= At_1^2 + 2Ct_1t_2 + Bt_2^2 + 2A't_1 + 2B't_2 + D \quad (3.10)$$

$$= B(t_2 - t_2^+)(t_2 - t_2^-), \quad (3.11)$$

where coefficients  $A, B, \dots, D$  are functions of the other integration variables. The inner integration over  $t_2$  and  $t_1$  has to be carried out over the region bounded by the condition  $\Delta_4 = 0$ , which in our case defines an ellipse. The integration were performed by using three different methods. In the simplest method we in order to get rid of the singularities at the end points of the  $t_2$  -integration removed  $\Delta_4$  by replacing the integration variable  $t_2$  by the variable  $u$  defined by

$$t_2 = \frac{t_2^+ + t_2^-}{2} + \frac{t_2^+ - t_2^-}{2} \cdot \sin u, \quad (3.12)$$

in terms of which the integration becomes

$$\int_{t_2^-}^{t_2^+} \frac{f(t_1, t_2)}{\sqrt{-\Delta_4}} dt_2 = \frac{4}{\sqrt{B}} \int_{-\pi/2}^{\pi/2} f(t_1, t_2(u)) du \quad (3.13)$$

After this we applied the Monte Carlo program MONTE [7] to compute the 4-fold integral. For checking we used two other programs were the  $t_2$  integration or both the  $t_2$  and  $t_1$  integrations were first made analytically and the MONTE was used for the rest.

The program of the third stage consisted of setting in the explicit expressions for the vertices and the numerical results for the integrals, and of summing the different contributions to get the total cross section.

We used the following symmetry relations for checking:

$$\sigma_{ij} = \sigma_{ji}^* \quad (3.14)$$

and

$$\sigma_{ij} = \sigma_{i_c j_c} \quad (3.15)$$

Here the  $\sigma_{ij}$  is the cross section contribution coming from the cross term of the amplitudes  $i$  and  $j$ , and  $i_c$  refers to the amplitude obtained from the amplitude of the index  $i$  by charge conjugation:

$$T_{i_c}(p_2, p_1) = C T_i^T(p_1, p_2) C^{-1} \quad (3.16)$$

From Table 2.1 we see that  $1_c = 6$  and  $3_c = 4$ , which gives e.g. the relations  $\sigma_{13} = \sigma_{46}$  and  $\sigma_{14} = \sigma_{36}$ . The derivation of relation (3.15) is based on the equation:

$$Tr\{T_{1C}(p_2, p_1) \not{p}_1 \overline{T_{2C}(p_2, p_1)} \not{p}_2\} = Tr\{T_1(p_1, p_2) \not{p}_1 \overline{T_2(p_1, p_2)} \not{p}_2\}_{p_1 \rightarrow p_2} \quad (3.17)$$

which follows from the definitions

$$\left\{ \begin{array}{l} C \gamma^\mu C^{-1} = -\gamma^{\mu T} \\ \gamma^0 \gamma^\mu \gamma^0 = (\gamma^\mu)^\dagger \\ C^{-1} = C^+ = C^T = -C \\ \bar{\Gamma} = \gamma^0 \Gamma^+ \gamma^0 \end{array} \right. \quad (3.18)$$

$$\begin{cases} \sigma_{11,11} = \sigma_{12,12} = \sigma_{11,12} = \sigma_{12,11} \propto s/4(M_1 M_2 M_3)^2 \\ \sigma_{11,13} = \sigma_{12,13} = \sigma_{13,11} = \sigma_{13,12} \propto -s/3(M_1 M_2 M_3)^2 \\ \sigma_{13,13} \propto s/2(M_1 M_2 M_3)^2. \end{cases} \quad (3.20)$$

Here we have dropped an overall factor and we have used the notation  $M_Z = M_3$  again. The result immediately reveals that the contributions from the diagrams d) and f) do not cancel each other at high energies although the contributions from the corresponding subdiagrams do. The compensation needed should come from the amplitudes 1 - 6 and interference terms of the amplitudes 11 - 13 with other amplitudes. We notice that the diagram f) and the corresponding amplitude 13 differ from all standard model counterparts, because it contains a vertex where a virtual scalar decays into another virtual scalar and a massive vector boson. From the equations (3.20) one can see that the amplitudes 11 and 12 would achieve a good high-energy behaviour also without the amplitude 13 if they would differ in their signs. We, however, were unable to find an error in our vertex calculation and so we keep the diagram f) and the signs as they are.

Further, three different methods were applied for the integration. In the first one the integrals of the partial 92 cross sections  $\sigma_{ij}$  ( $i, j = 1, \dots, 13; i < j$ ) were carried separately and the results were multiplied by the coefficients of the amplitudes. In most cases this gave enough accurate results, but for some numerical reason it radically overestimated especially the contribution from the part 7+9, when the energy approached 10 TeV.

In the second method the amplitudes were grouped into the sets 1+3+4+6, 2+5, 7+9, 8+10, 11+12+13, which corresponds to our subdiagram idea. The squares of the sets and the cross terms of the different sets were integrated separately with amplitudes multiplied by their respective coefficients before integration. This method allowed a faster computation and the result were expected to be more accurate than in the first method. For the part 11+12+13 we also had a special routine based on the single numerical integration by the MATHEMATICA. It run accurately also at very high energies (1000 TeV) and provided a valuable checking for our analytical results and for our other programs. The contributions arising from our partition behaved at high energies in the expected way. We liked this method best, because it was both illuminating and accurate.

The last method was based on a single 4-fold integration where the multiplication of the amplitudes with their coefficients as well as the summation of all the 92 terms were done under integration. The information concerning various separate contributions to the cross section was lost in this method, but using a high precision in the computation this should give the most accurate result. We have used this method only at the energy of 2 TeV and the result coincides with the results of the two first methods.

In Fig 4.1 we present the contributions from the amplitude sets to the total cross section in the energy region of 1 - 5 TeV. Here the sets 7+9 and 8+10 have been summed into a single contribution. The characteristic feature is the form of a fan where the absolute values of the contributions increase with the energy but some of them are positive and the other are negative. The contribution from 2+5 is not presented, because it is negligible due to the smallness of the coupling between the light Z-boson and the heavy neutrinos.

Figure 4.2 gives the total cross section, which is amazingly small. The cancellation of various contributions is very effective, which have also been the main reason for the numerical problems we met in our computations. A tiny irregularity in the smooth curve in the region of 1 - 1.5 TeV is probably caused by the masses which are near to this region. The stile rise of the curve just below 5 TeV could be a first mark of the singularity at 10 TeV. These irregularities have not studied closer in this work where the main purpose was to get a reliable estimation for the magnitude of the cross section in the region of 1 - 2 TeV. The details will be cleared later by letting the mass parameters vary.

There is also another disturbing feature in Fig 4.2, namely, that the curve rises in the whole region. We would expect a stile rise from the threshold to the maximum and then a more or less slow decrease to zero with a peak at the mass of  $\Delta^{--}$ . The decrease before the pole can, however, be hindered by the pole, if the mass of  $\Delta^{--}$  is sufficiently close to the threshold energy. We think this the case in Fig 4.2, but we have to leave the checking of this for a further study, where we will use a faster computer.

In Figures 4.3 - 4.4 we present the same entities as in Figures 4.1 - 4.2 but now in the energy region of 2 - 100 TeV. In these high-energy pictures the mass of the  $\Delta^{--}$  is taken to be 0.8 TeV. So we are free of singularities and are able to see whether the cancellation of the various contributions really happen. The Fig 4.3 is very similar to Fig 4.1 but some contributions have changed their signs, because we are now above the pole of the  $\Delta^{--}$ . The Fig 4.4 shows the sum of all the partial cross sections and the cancellation is convincing below 20 TeV. Above this energy the cross section begins to vary accidentally due to a too low numerical accuracy. The first three digits of the partial cross sections cancel and the result now strongly hints that there is a clear maximum in the cross section. There is, however, already inner cancellations in the partial cross sections of our sets. In Fig 4.5 we show an example where the contributions cancel in several digits. Here as usually in our Figures and Tables the contribution  $\sigma_{ij}$  includes  $\sigma_{ji}$  if  $i \neq j$ . The partial cross sections coming from our sets of amplitudes are remains from inner cancellations in the sets and they cancel further when we sum the partial cross sections. Therefore we have to wait for results

# Bibliography

- [1] E. Byckling and K. Kajantie, *Particle kinematics*, Wiley, Bristol 1973
- [2] N.G. Deshpande, J.F. Gunion, B. Kayser, and F. Olness, Phys. Rev. D44, 837 (1991)
- [3] D. Dicus, D. Karatas, and P. Roy, Phys. Rev. D44, 2033 (1991)
- [4] J. Gluza and M. Zralek, Phys. Rev. D45, 1693 (1992)
- [5] J.F. Gunion, J. Grifors, A. Mendes, B. Kayser, and F. Olness, Phys. Rev. D40, 1546 (1989)
- [6] J.F. Gunion, a talk in the *2nd International Workshop on Physics and Experiments at Linear  $e^+e^-$  Colliders*, Waikoloa, Hawaii, April 1993
- [7] S. Gupta, *Subroutine Monte*, A Monte Carlo program
- [8] C. A. Heusch, a talk in the *2nd International Workshop on Physics and Experiments at Linear  $e^+e^-$  Colliders*, Waikoloa, Hawaii, April 1993
- [9] C. A. Heusch and P. Minkowski, CERN-TH.6606/92, SCIPP 93/07, BUTP-93/14
- [10] J. Hewett, a talk in the *2nd International Workshop on Physics and Experiments at Linear  $e^+e^-$  Colliders*, Waikoloa, Hawaii, April 1993
- [11] G. P. Lepage, *Subroutine Vegas*, A Monte Carlo program, the algorithm described in J. Comp. Phys. 27, 192 (1978)
- [12] J. Maalampi, A. Pietilä and J. Vuori, preprint HU-TFT-92-10 (1992), Nucl. Phys. B381, 544 (1992)
- [13] J.C. Pati and A. Salam, Phys. Rev. D10, 275 (1974); R.N. Mohapatra and J.C. Pati, Phys. Rev. D11, 566, 2558 (1975) G. Senjanovic, Nucl. Phys. B153, 334 (1979)
- [14] A. Pietilä, J. Maalampi, and J. Vuori, Laboratory report Turku-FL-R9, Department of Physics, University of Turku, Finland (1992); J. Maalampi, A. Pietilä, and J. Vuori, Phys. Lett. B297, 327 (1992)
- [15] A. Pietilä and J. Maalampi, Laboratory report Turku-FL-R10, Department of Physics, University of Turku, Finland (1992); J. Maalampi and A. Pietilä, Z. Phys. C59, 257 (1993)
- [16] T. G. Rizzo, Phys. Lett. B116, 23 (1982); A talk in the *2nd International Workshop on Physics and Experiments at Linear  $e^+e^-$  Colliders*, Waikoloa, Hawaii, April 1993; ANL-HEP-CP-93-24

# Figures of Chapter 4

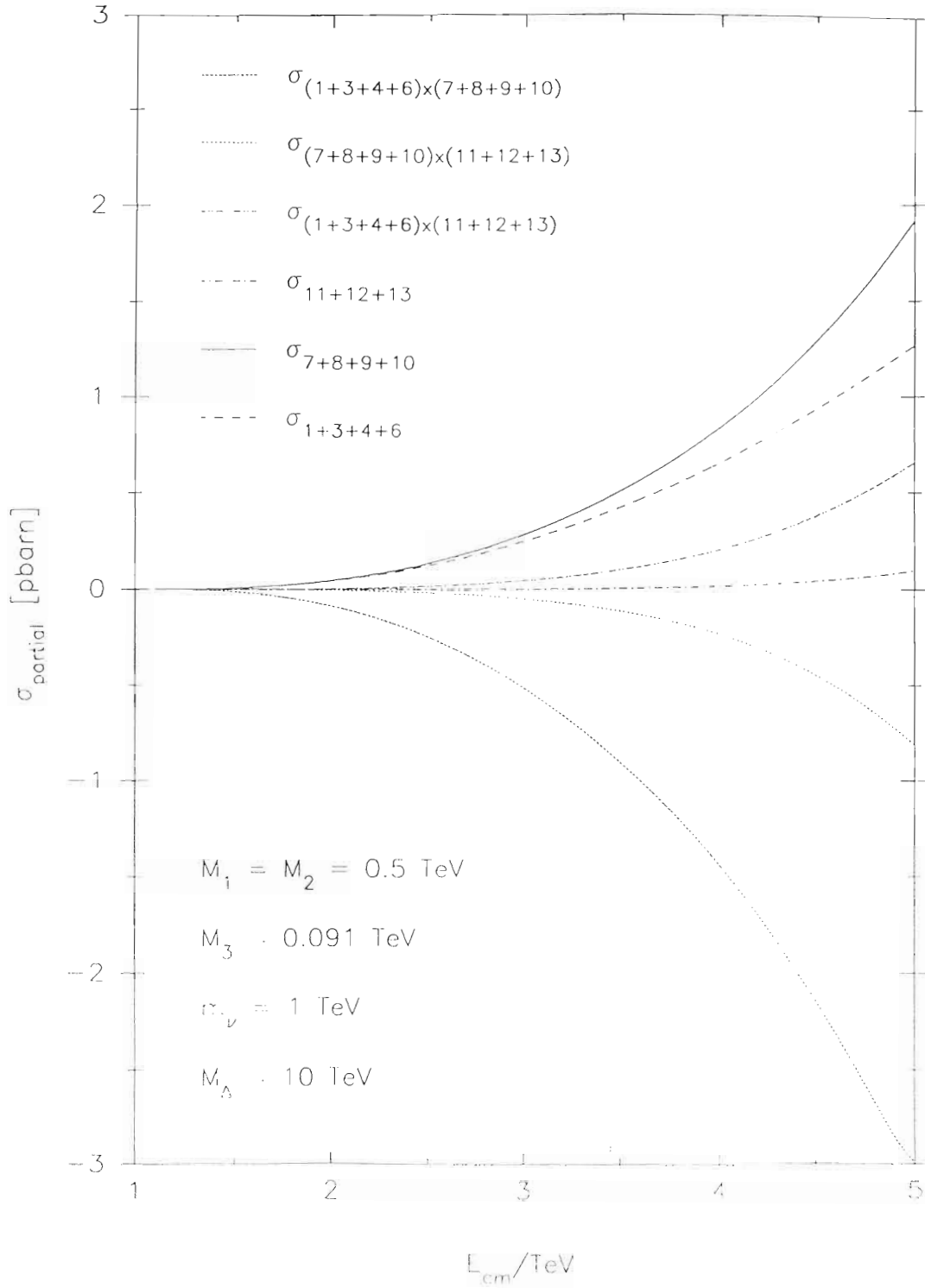


Fig 4.1

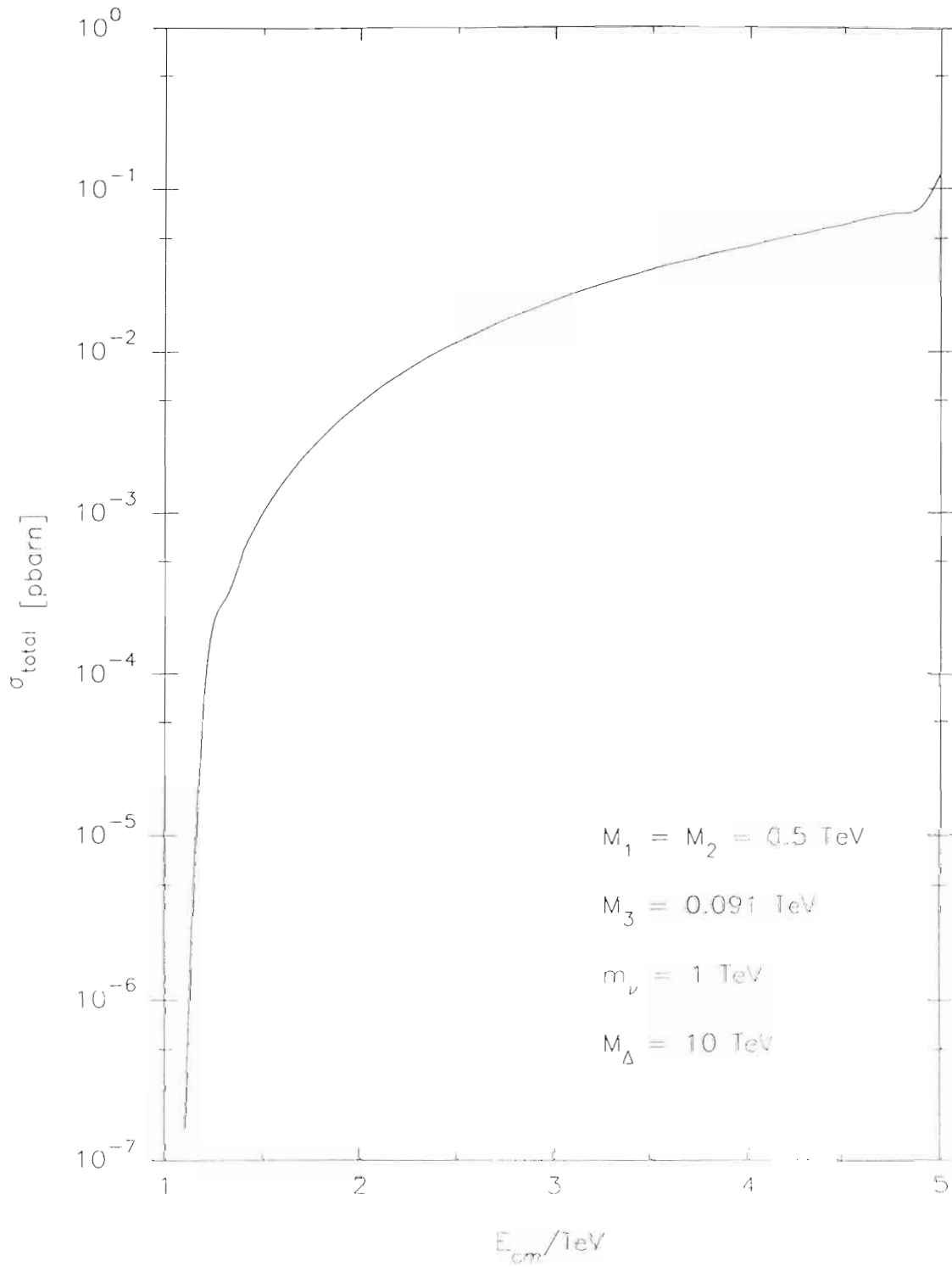


Fig 4.2

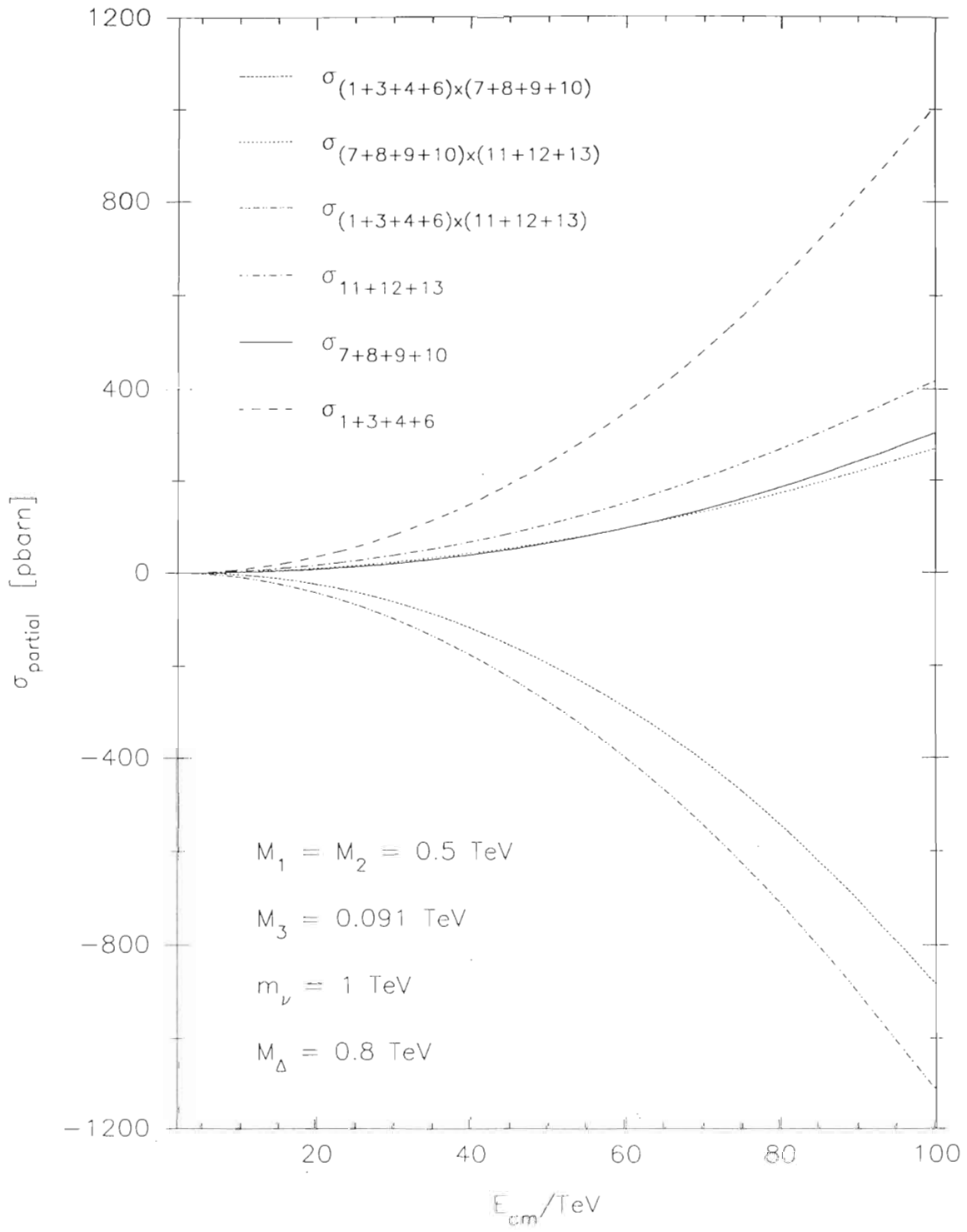


Fig 4.3

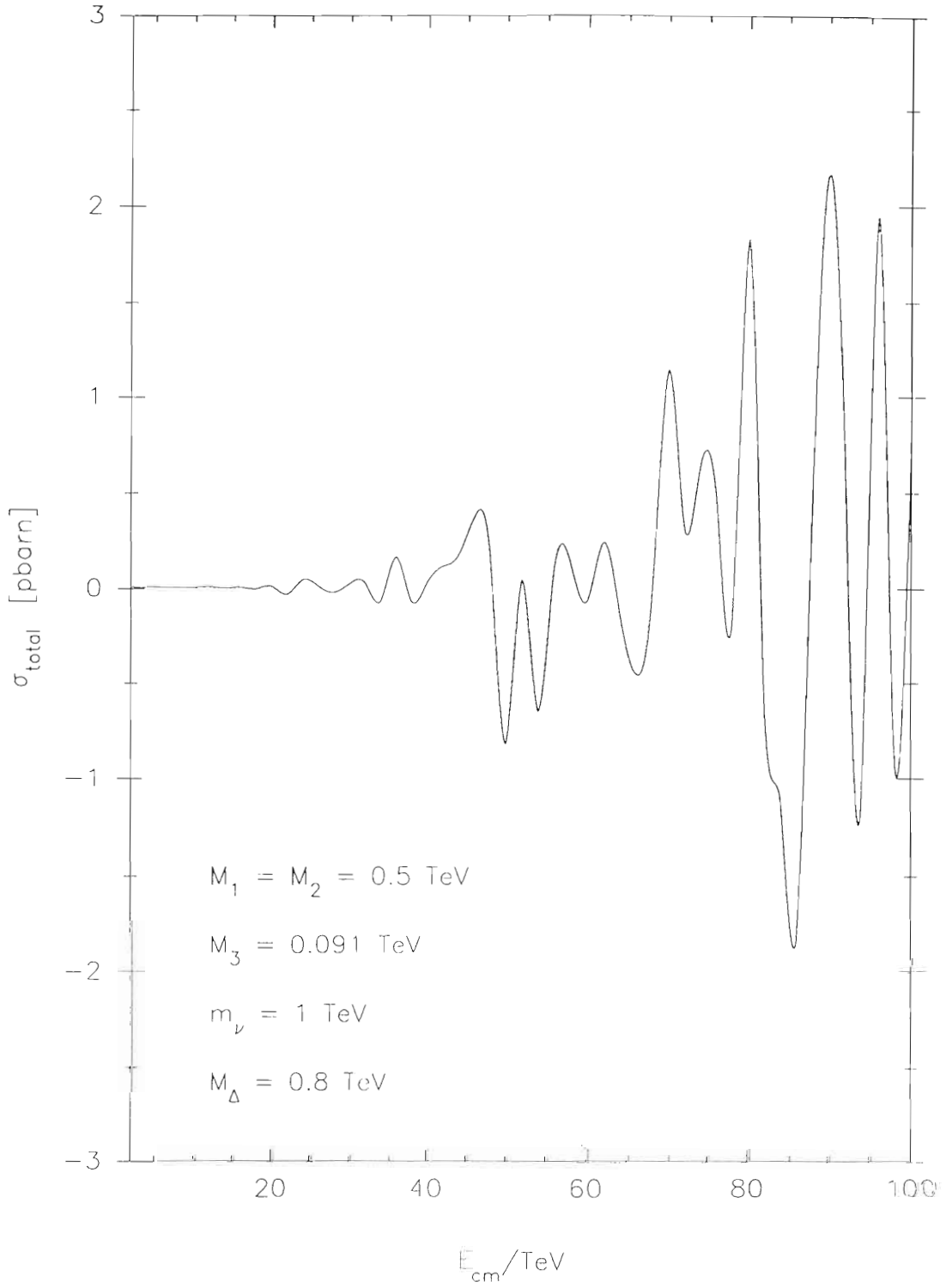


Fig 4.4

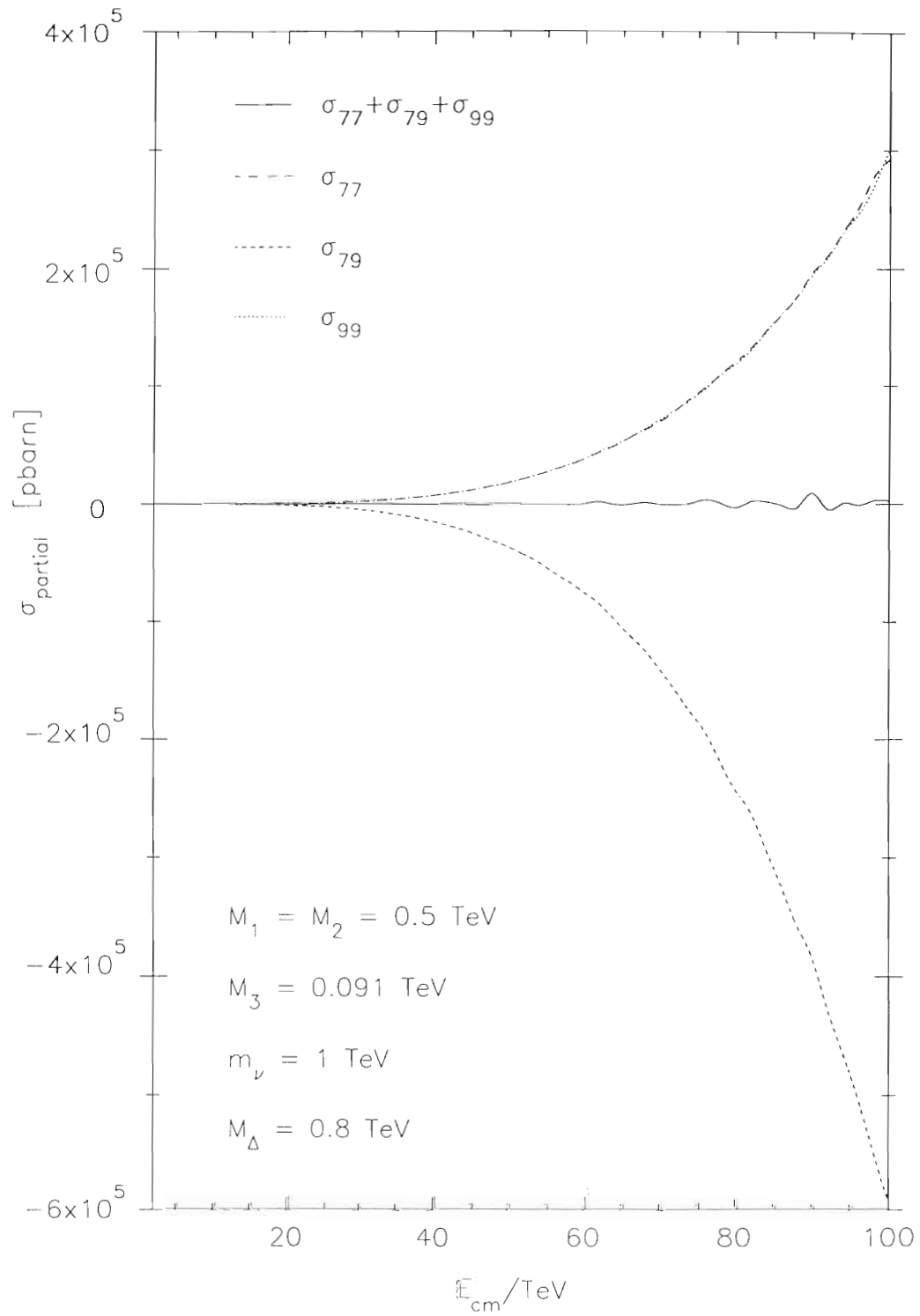


Fig 4.5